AALBORG UNIVERSITY

Performance Comparison of Reconstruction Algorithms in Discrete Blind Multi-Coset Sampling

Grigoryan, Ruben; Arildsen, Thomas; Tandur, Deepaknath; Larsen, Torben

Performance Comparison of Reconstruction Algorithms in Discrete Blind Multi-Coset Sampling

Ruben Grigoryan, Thomas Arildsen, Deepaknath Tandur*, Torben Larsen

Department of Electronic Systems, Aalborg University, Aalborg, Denmark

{rug, tha, tl}@es.aau.dk

*Agilent Technologies, Belgium

Abstract—*This paper investigates the performance of different reconstruction algorithms in discrete blind multi-coset sampling. Multi-coset scheme is a promising compressed sensing architecture that can replace traditional Nyquist-rate sampling in the applications with multi-band frequency sparse signals. The performance of the existing compressed sensing reconstruction algorithms have not been investigated yet for the discrete multi-coset sampling. We compare the following algorithms – orthogonal matching pursuit, multiple signal classification, subspace-augmented multiple signal classification, focal under-determined system solver and basis pursuit denoising. The comparison is performed via numerical simulations for different sampling conditions. According to the simulations, focal under-determined system solver outperforms all other algorithms for signals with low signal-to-noise ratio. In other cases, the multiple signal classification algorithm is more beneficial.*

Keywords—*compressed sensing, multi-band signals, multi-coset sampling, multiple-measurement vectors.*

I. INTRODUCTION

Bandpass and multi-band signals can be successfully sampled at frequencies below the Nyquist-Shannon limit, so called sub-Nyquist sampling [1]. For this type of signals the minimum sampling rate depends on the accumulated bandwidth rather than the highest frequency component as in the classical Nyquist-Shannon-Kotelnikov theorem. Nonuniform periodic sampling is one of the method for sub-Nyquist sampling. This strategy can be implemented with parallel sampling channels each of them containing an analog-to-digital converter (ADC). The ADCs perform measurements at different moments of time. Such a scheme is called a multi-coset sampling scheme (see Fig. 1) [2]. The problem of sub-Nyquist sampling of non-baseband signals has been discussed in a number of papers [2], [3], [4], [5], [6].

Consider multi-band signals. When the positions of bands in a signal are known in advance (non-blind sampling) the reconstruction can be performed with specially designed filters [3], [4]. In [2] Feng and Bresler introduced blind sampling where the positions of bands are unknown prior to sampling. Blind sampling can be seen as a compressed sensing problem for multiple-measurement vectors (MMV) [6].

The method proposed by Feng and Bresler allows to directly reconstruct a continuous input signal without discretization. This approach avoids the negative discretization issues such as the need for block processing, windowing and spectrum leakage. The same idea was used in [5], [7]. However, the purpose of some applications, e.g. spectrum analyzers, is to
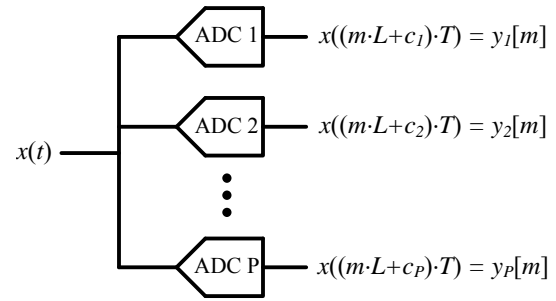

Fig. 1. Multi-coset sampling scheme [2].

evaluate the frequency spectrum rather than to reconstruct the continuous input signal in time domain. For these applications the discrete Fourier transform (DFT) of a sequence of the samples of an input signal is computed. Thereby, discretization is introduced. From this perspective it is interesting to investigate the quality of the DFT evaluation when the traditional Nyquist-rate sampling is replaced by compressed sensing with the multi-coset scheme. i.e. the discrete multi-coset sampling. To date, such a discrete approach has not been considered. Throughout the paper, by signal reconstruction we mean the evaluation of the DFT of a sequence of samples. We wish to determine in which cases the multi-coset sampling can replace traditional Nyquist-rate sampling and extend the functionality of the existing sampling applications. For that purpose the performance of different reconstruction algorithms should be evaluated.

In multi-coset sampling the bandwidth of a single ADC should be higher than the bandwidth of the input signal. In [7] the modified multi-coset sampling scheme, named modulated-wideband converter, was presented. Modulated-wideband converter has a premixing stage before analog-to-digital conversions which allows using ADCs with a relatively low input bandwidth. The price for that is a more complicated front-end. However, an 80 channels time-interleaved ADC implemented as a single integrated circuit already exists [8]. The multi-coset scheme can be made from the time-interleaved scheme by simply removing some of the parallel channels. So, there are no technological obstacles in implementing multi-coset sampling.

In order to make one more step toward implementation of compressed sensing acquisition systems for real-life applications, we numerically investigate the quality of the DFT

evaluation when the Nyquist-rate sampling is replaced by the sub-Nyquist multi-coset sampling. The objective is to investigate the relations between the number of sampling channels (an average sampling rate), the number of bands in signals, widths of bands, power of noise in signals on one side and reconstruction distortion on another. The reconstruction quality is evaluated by comparing the two DFT sequences. One is obtained with the Nyquist-rate sampling and is used as a reference. The second is obtained with the multi-coset sampling. We consider the following reconstruction algorithms: orthogonal matching pursuit for MMV (M-OMP) [9], multiple signal classification (MUSIC) [6], subspace-augmented MUSIC (SA-MUSIC) [10], basis pursuit denoising for MMV (M-BPDN) [11], [12] and focal underdetermined system solver for MMV (M-FOCUSS) [9]. To date these algorithms have not been compared in the application of discrete multi-coset sampling. M-OMP and M-FOCUSS were described and compared in [9] but BPDN, MUSIC and SA-MUSIC were not considered. In [13] the authors proposed a new way of finding the solution to the MMV equation by solving a set of randomly formed singular-measurement vector problems. However, the success of this method depends on whether the number of random sub-problems is large enough. All the cases considered in [13] were noiseless and MUSIC-like algorithms were not considered.

The main contribution of this paper is that we formulate the discrete multi-coset approach and compare the performance of different reconstruction algorithms for the evaluation of the DFT. Our discrete multi-coset approach links together the unknown DFT of the sequence of samples of an input signal and the known DFTs of samples from sensing channels.

The outline is as follows. In Section II we review a multi-coset sampling scheme, describe discrete multi-coset sampling, test signals and performance measures. Algorithms that are used for the reconstruction are specified in Section III. In Section IV we present the complete simulation setup and the simulation results. Conclusions are stated in Section V.

II. MULTI-COSET SCHEME, TEST SIGNALS AND PERFORMANCE MEASURES

A. Multi-coset scheme

The main idea of the multi-coset scheme is to use multiple ADCs with a low sampling frequency rather than one that operates at a high frequency. As can be seen on Fig. 1, a multi-coset scheme consists of P parallel sampling channels. The ADCs in these channels perform sampling of an input signal $x(t)$ at different moments of time specified by the set of time shifts $C = \{c_1, \ldots, c_P\}$, $c_p \in \{0, 1, \ldots, L - 1\}$, for channel $p = \{1, \ldots, P\}$. The positive integer L is called the multi-coset sampling period, $1 \leq P < L$. The combination of L and C denoted by (L, C) is called a multi-coset sampling pattern [6]. The time period $T = 1/(2 \cdot f_{\max})$ is the Nyquist sampling period and all the frequency components in an input signal are less than $f_{\max}$. In this paper we do not consider quantization effects.
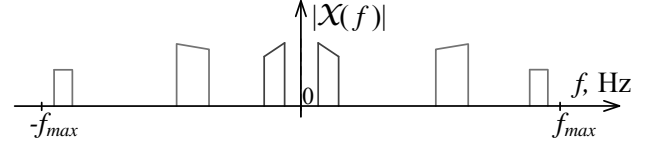
(a) Absolute values of the discrete-time Fourier transform of the three-band signal $x(t)$.
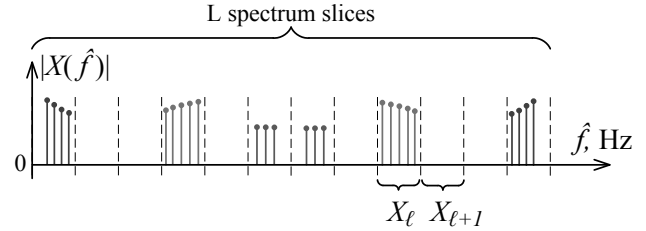
(b) Absolute values of the DFT coefficients of the three-band signal $x(t)$ sampled at the rate $1/T$, $\hat{f}$ denotes the discrete frequency.

Fig. 2. Illustration of the Fourier transform and the discrete Fourier transform of the sequence of samples of the three-band signal $x(t)$.

Assume that $\mathcal{X}(f), f \in (-f_{\max}, f_{\max})$, is the unknown discrete-time Fourier transform of an input signal $x(t)$ (see Fig. 2(a)). In the multi-coset scheme the relation between the input and the outputs is as follows [5], [6]:

$$\mathbf{y}(f) = \mathbf{A} \cdot \mathbf{x}(f) \tag{1}$$

$$\mathbf{y}(f) = [y_1(f), \ldots, y_P(f)]^{\mathrm{T}}, \ \mathbf{x}(f) = [x_1(f), \ldots, x_L(f)]^{\mathrm{T}}$$

where $f \in F_0 = [0, \frac{1}{L \cdot T})$, $y_i(f) \in \mathbb{C}$ is the known discrete time Fourier transform of $y_i[m]$, $m \in \mathbb{Z}^+$, $x_\ell(f) = \mathcal{X}(f + \frac{\ell}{LT}) \in \mathbb{C}$ is the ℓth slice upon slicing $\mathcal{X}(f)$ into L equal-sized parts. The measurement matrix $\mathbf{A} \in \mathbb{C}^{P \times L}$ is given by:

$$A_{i,\ell} = \frac{1}{L \cdot T} \exp\left[j \frac{2\pi}{L} \cdot c_i \cdot \ell\right]. \tag{2}$$

In (1) f is a continuous variable. Therefore this equation describes an infinite dimensional problem [6], [13]. In [2] the authors proposed a method that reduces the infinite dimensional problem to the finite dimensional MMV by computing the correlation matrix of the interpolated ADCs' output sequences. This allows to reconstruct the continuous input signal without discretization. However, there are practical applications where the DFT of the sequence of samples of an input signal is computed rather than the time-domain reconstruction, e.g. spectrum analyzers. From this perspective it is interesting to evaluate how the DFT of a multi-band frequency sparse signal can be estimated with the multi-coset sampling scheme. Denote by $X(\hat{f}) \in \mathbb{C}^K$ the DFT of the sequence of length K obtained by uniform sampling $x(t)$ with the sampling rate $1/T$. The discrete multi-coset problem can be formulated as follows:

$$\widehat{\mathbf{Y}} = \mathbf{A}\mathbf{X} \tag{3}$$

$$\widehat{\mathbf{Y}} = \begin{pmatrix} Y_1 \\ \vdots \\ Y_P \end{pmatrix} \circ \begin{pmatrix} \alpha_{1,1} & \dots & \alpha_{1,M} \\ \vdots & \ddots & \vdots \\ \alpha_{P,1} & \dots & \alpha_{P,M} \end{pmatrix}$$

$$\alpha_{p,m} = \exp\left[\frac{-2\pi j \cdot c_p \cdot m}{K}\right], \ p \in \{1, \dots, P\}, \ m \in \{1, \dots, M\}$$

$$\mathbf{X} = \begin{pmatrix} X_1 \\ \vdots \\ X_L \end{pmatrix} = \begin{pmatrix} X(1) & \dots & X(M) \\ \vdots & \ddots & \vdots \\ X((L-1)\cdot M + 1) & \dots & X(L \cdot M) \end{pmatrix}$$

where $\widehat{\mathbf{Y}} \in \mathbb{C}^{P \times M}$ and $\mathbf{X} \in \mathbb{C}^{L \times M}$, $\circ$ denotes Hadamard product (element-wise multiplication). $Y_P \in \mathbb{C}^M$ is the known DFT of the output sequence of the pth channel, i.e $Y_p = \mathcal{F}_{\text{DFT}}(y_p[1, 2, \dots, M])$, $\mathcal{F}_{\text{DFT}}$ denotes DFT. $X(j)$ is the jth element of $X(\hat{f})$. Then the matrix $\mathbf{X} \in \mathbb{C}^{L \times M}$ is formed by slicing and rearranging the unknown DFT transform $X(\hat{f})$, $X_\ell \in \mathbb{C}^L$ is the ℓth slice of $X(\hat{f})$ (see Fig. 2(b)). We assume that the total number of the observed samples of $x(t)$ equals to $K = L \cdot M$. The coefficients $\alpha_{i,m}$ are introduced to compensate the time shift of the mth DFT bin in the pth sampling channel. The multi-coset sampling for discrete signals can be done in three steps:

1) Take M samples from each ADC;
2) Take DFTs of the obtained sequences;
3) Multiply each DFT bin by the corresponding time shift multiplier;

Equation (3) establishes the relation between the DFT transforms of the sequences of samples of an individual channel and the DFT transform of the input signal. This interpretation of the multi-coset sampling differs from the original idea that is to reconstruct a continuous input signal [2], [6], [5]. If $\mathbf{X}$ can be uniquely defined from (3) given $\widehat{\mathbf{Y}}$, the traditional Nyquist-rate sampling can be replaced by the sub-Nyquist multi-coset sampling in applications where DFT is needed. To our best knowledge, this discrete approach has not been used in the existing publications. Discretization introduces some undesirable features such as spectrum leakage, the need for block processing, windowing effects etc. At the same time, all these negative effects appears in the Nyquist-rate sampling as well.

Each column of the unknown matrix $\mathbf{X}$, a source vector, has the corresponding column of the known matrix $\widehat{\mathbf{Y}}$, the measurement vector. This is why (3) is named the multiple-measurement vectors problem [9]. The task of a reconstruction algorithm is to find the unknown $\mathbf{X}$ based on the known $\widehat{\mathbf{Y}}$ and $\mathbf{A}$. Recall that $P < L$. Therefore, in the general case of arbitrary $\mathbf{X}$ the system of linear equations (3) is under-determined, so it does not have a unique solution. For the signal measurement application this means that the sampled signal can not be uniquely reconstructed. However, the rows $X_\ell \in \mathbb{C}^L$ of $\mathbf{X}$ are slices of the $X(\hat{f})$ (see Fig. 2(b)). If $X(\hat{f})$ only has few non-zero bands, the matrix $\mathbf{X}$ only has

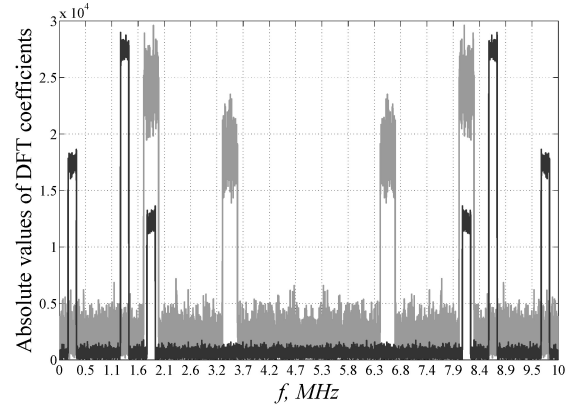Fig. 3. Illustration of the test signals. Black line – the signal with $N=3$, $\Omega = 0.1$, SNR = 20 dB, grey line – the signal with $N=2$, $\Omega = 0.12$, SNR=10 dB, $f_{\max} = 5$ MHz. Test signals consist of $K = L \cdot M$ samples. Dashed lines show the positions of the frequency slices.

few non-zero (whole or partly) rows. Under this assumption, blind multi-coset sampling for discrete multi-band signals becomes the compressed sensing problem. It was proven that a unique solution to (3) exists under certain conditions. Various theoretical aspects of compressed sensing, such as require-ments for the measurement matrix, the necessary number of measurements, robustness to noise etc. are discussed in [14] and its references.

Denote by S a set of indices of non-zero rows of $\mathbf{X}$. This set is called the support of $\mathbf{X}$ and indicates the non-zero frequency slices. The matrix $\mathbf{X}_S$ is formed by selecting the rows of $\mathbf{X}$ with indices S and $\mathbf{A}^S$ is formed by selecting the columns of $\mathbf{A}$ with the same indices S. Then (3) is reduced to [5]:

$$\widehat{\mathbf{Y}} = \mathbf{A}^S \mathbf{X}_S \tag{4}$$

The properties of the matrix $\mathbf{A}^S$ affect the performance of the sampling system. The reconstruction fails if $\mathbf{A}^S$ does not have full column rank. In the presence of noise a high condition number of $\mathbf{A}^S$ will also lead to the reconstruction failure. It is of particular interest to select the sampling pattern (L, C) that yields a well-conditioned $\mathbf{A}^S$ for all possible variations of the support S. For our simulation we select the sampling pattern for each number of the sampling channels by searching over the all possible combinations and analysis of the condition numbers [6].

B. Test signals and performance measures

The level of frequency sparsity of a signal can be quantified by the spectral occupancy ratio Ω:

$$\Omega = \frac{\lambda(\text{supp}\langle (X(\hat{f}))\rangle)}{\lambda([0, f_{\max}])}, \ \Omega \in [0, 1] \tag{5}$$

$\text{supp}\langle\cdot\rangle$ is the support of $X(\hat{f})$, which is the set of frequency points where $X(\hat{f})$ is nonzero, $\lambda(\cdot)$ denotes the Lebesgue measure. In our case the Lebesgue measure is equal to the joint length of frequency bands. We assume that $X(\hat{f})$ does

not contain noise when we calculate the value of Ω, so that broadband noise does not affect it. Denote by N the number of bands in a signal. Then Ω and N describe the structure of the signal (see Fig. 3).

To evaluate the performance of the reconstruction algorithms we use multi-band test signals with different parameters. We vary occupancy ratio, number and positions of bands and power of noise in signals. Frequency bands are formed via $\text{sinc}(\cdot)$ functions in the time domain and always centered at the middle of the frequency slices. Signals are real-valued. We use the support reconstruction ratio as one of the performance measure:

$$R = \frac{\text{Number of correctly found support sets}}{\text{Number of test signals}}. \quad (6)$$

Support reconstruction ratio shows how well a reconstruction algorithm identifies the positions of bands in a signal.

As for the second performance measure we use *relative root mean square* (RRMS) value:

$$\text{RRMS} = \sqrt{\frac{\sum_{i=1}^{K}(\widehat{X}(i) - X(i))^2}{\sum_{i=1}^{K} X^2(i)}} \geq 0 \quad (7)$$

where $X(i)$ and $\widehat{X}(i)$ are original and estimated DFT coefficients of the test signal, $K = L \cdot M$ is the total number of DFT coefficients. In case of Nyquist-rate sampling RRMS is always equal to 0.

To simulate noisy environment we add white Gaussian noise to the test signals. The power of noise corresponds to the specified Signal-to-Noise Ratio (SNR) as illustrated in Fig. 3.

$$\text{SNR} = 10 \cdot \log_{10}\left(\frac{\text{P}_{\text{signal}}}{\text{P}_{\text{noise}}}\right) \quad (8)$$

where P_{signal} is power of a clean signal, P_{noise} is power of noise. Thus, we introduce noise folding:

$$\widehat{\mathbf{Y}}_N = \mathbf{A}\left(\mathbf{X} + \mathbf{N}\right) \quad (9)$$

where $\widehat{\mathbf{Y}}_N \in \mathbb{C}^{P \times M}$ is the matrix of measurements of a noisy signal and $\mathbf{N} \in \mathbb{C}^{L \times M}$ is the matrix that corresponds to broadband noise. Elements of $\mathbf{N} \in \mathbb{C}^{L \times M}$ are independent and identically distributed from the Gaussian distribution.

III. RECONSTRUCTION ALGORITHMS

We consider the following algorithms that are used in compressed sensing applications: 1) Orthogonal Matching Pursuit for MMV – M-OMP [9], 2) MUltiple Signal Classification – MUSIC [6], 3) Subspace Augmented-MUSIC [10], 4) FOCal Underdetermined System Solver for MMV – M-FOCUSS [9], 5) Basis Pursuit Denoising for MMV – M-BPDN [11], [12]. The MUSIC algorithm was used by Feng and Bresler in [2] when they proposed multi-coset blind sampling. SA-MUSIC is further development of MUSIC. The other three algorithms are used to solve general MMV problems. The detailed description of the reconstruction algorithms can be found in the corresponding references.

Algorithms 1–3 show the best performance when the number of non-zero rows of $\mathbf{X}$ is known prior to the reconstruction. Otherwise we have to estimate the number of non-zeros. However, the precision of this estimation is based on many factors: level of noise in a signal, width of bands in a signal, dynamic range of the input signal etc. In our simulation we assume that the number of non-zeros is known prior to the reconstruction, otherwise the performance of the reconstruction algorithm will be limited by the algorithm estimating this number.

In additional to the general regularized M-FOCUSS we implement a modification M-FOCUSS* that takes the number of non-zero rows of $\mathbf{X}$ as an input parameter and returns the indices of non-zero frequency slices. That allows to compare M-FOCUSS* to algorithms 1–3 in terms of the support reconstruction ratio.

We use our own implementations of the reconstruction algorithms except M-BPDN [11], [12]. Signal subspace estimation in SA-MUSIC is performed by thresholding eigenvalues. M-FOCUSS was implemented with Tikhonov regularization [9], the regularization parameter was picked empirically. The internal parameter of M-FOCUSS was set to 0.8 as it gives good tradeoffs between the sparsity of the solution and the convergence speed [9].

Signal reconstruction with M-OMP, MUSIC, SA-MUSIC and M-FOCUSS* is done in two steps. The first step is to find the frequency support S. Different algorithms do it in different ways. The second step is to solve the determined system (4). This step is the same for all these algorithms. So, the performance of M-OMP, MUSIC, SA-MUSIC and M-FOCUSS* can be compared in terms of the support reconstruction ratio R. M-FOCUSS and M-BPDN algorithms reconstruct a signal directly. Theirs performance is compared in terms of the RRMS values.

M-FOCUSS* and M-FOCUSS are initialized with the least square solution. For the algorithms $1, 2$ the correlation matrix $\mathbf{Q} = \widehat{\mathbf{Y}}_N \widehat{\mathbf{Y}}_N^H$ is computed. Algorithms 3–5 are applied directly to (9).

IV. SIMULATION

A. Simulation setup

For our simulations we use the multi-coset scheme with $L = 19$. Sampling patterns with a prime L yields to full column rank matrices $\mathbf{A}_S$ [5]. We vary the number of sampling channels from 1 to 19. Three types of sampling patterns are used: 1) optimal sampling patterns – patterns that are selected by exhaustive search for the lowest condition numbers, 2) random generated patterns, 3) bunched sampling patterns – $C = \{1, 2, \ldots, P\}$.
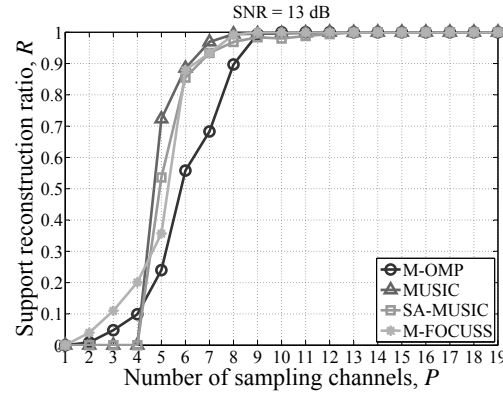
We created signals with different parameters. For one set of parameters we create 1000 random signal instances. Variation of parameters: $N = \{1, 2, 3, 4\}$, $\Omega = \{0.05, 0.10, 0.15, 0.2\}$, SNR $= \{30, 16, 13, 10, 6\}$ dB. Positions of bands are picked randomly but always in the middle of frequency slices.
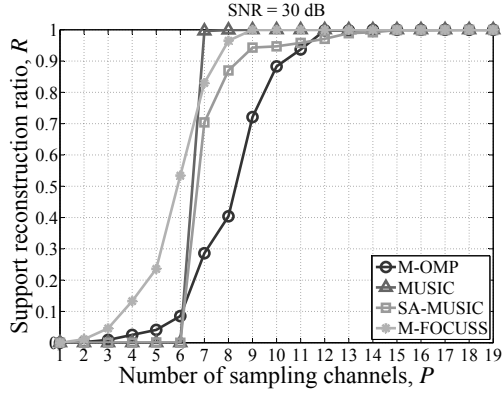
(a) $N = 3$, $\Omega = 0.15$, SNR=30 dB.
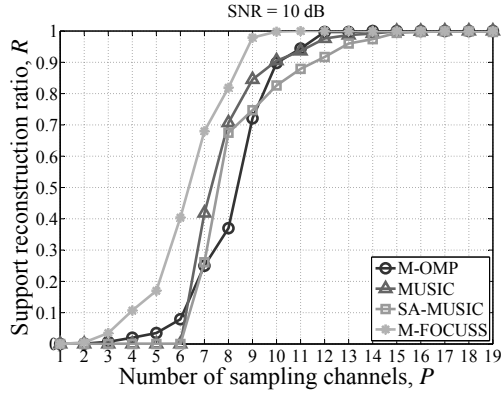
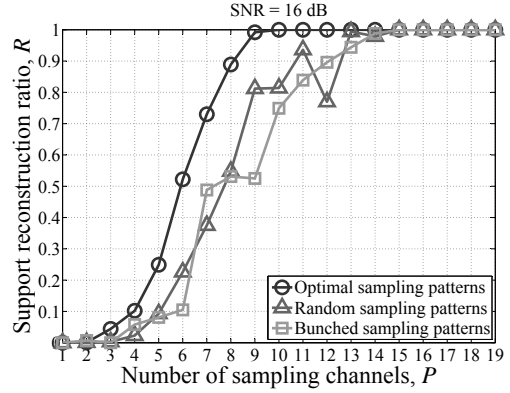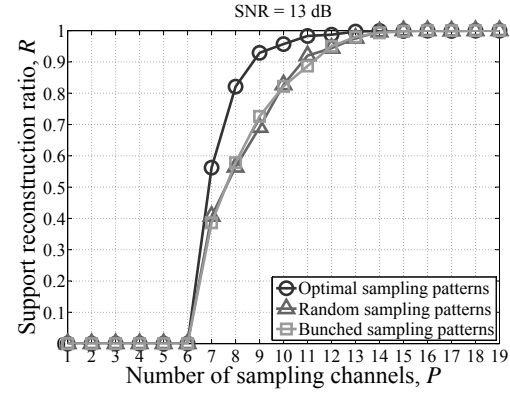(b) $N = 3$, $\Omega = 0.15$, SNR=10 dB.

(c) $N = 2$, $\Omega = 0.10$, SNR=13 dB.

Fig. 4. Empirical reconstruction rate with M-OMP, MUSIC, SA-MUSIC and M-FOCUSS* vs the no. of sampling channels. Optimal sampling patterns are used.

This gives control over the support of $\mathbf{X}$. Amplitudes of bands are picked within the 20 dB dynamic range. All bands have the same width. Bands do not overlap. Test signals are stored in files. This allows to run simulations for different reconstruction algorithms independently. M-OMP, MUSIC, SA-MUSIC and M-FOCUSS* take the number of non-zero frequency slices as an input parameter. M-BPDN and M-FOCUSS run without any prior information about the signals. The algorithms are validated by sampling and reconstructing test signals without noise. The source code used for the simulation is available at

(a) M-OMP, $N = 2$, $\Omega = 0.10$, SNR=16 dB.

(b) MUSIC, $N = 3$, $\Omega = 0.15$, SNR=13 dB.

Fig. 5. Empirical reconstruction rate with the selected algorithms for different types of the sampling patterns vs the no. of sampling channels.

http://www.sparsesampling.com/discretemulticoset.

B. Simulation results

Some of the simulation results are presented in Fig. 4–6. We do not include all the simulation results because of the limited paper space. However, the presented plots allow to make the correct conclusions as they preserve the tendency of behaviors of the reconstruction algorithms. Convergence analysis has shown the stability of the obtained data. For signals with a high SNR, MUSIC has the highest reconstruction rate (see Fig. 4(a)) – reconstruction rate 1 is obtained with the 7 channels while other algorithms require more sampling channels. However, M-FOCUSS* outperforms the MUSIC algorithm in case of a low SNR. As can be seen in Fig. 4(b) the reconstruction rate 1 for M-FOCUSS* is achieved with 10 sampling channel and for MUSIC with 12 channels.

SA-MUSIC is a further development of MUSIC that overcomes some restrictions of the original algorithm. But on Fig. 4 we see that the performance of SA-MUSIC is lower than the performance of MUSIC. The reason for this is the thresholding approach for the estimation of the signal subspace in SA-MUSIC [10]. If the signal subspace is not correctly estimated then the whole reconstruction fails. The thresholding parameter should be picked for each set of signal's parameters.
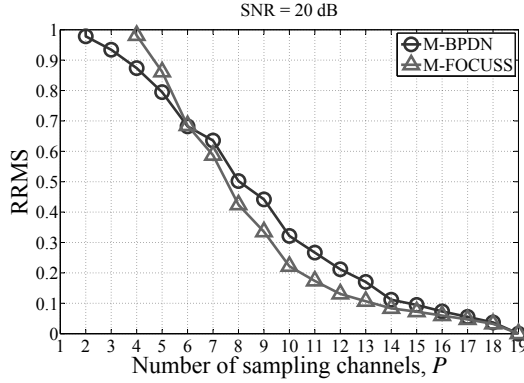
Fig. 6. RRMS error with M-BPDN and M-FOCUSS vs the no. of sampling channels, $N = 4$, $\Omega = 0.16$, SNR=20 dB. Optimal sampling patterns are used.

The M-OMP algorithm has the lowest reconstruction rate. However, the reconstruction performance of OMP is less sensitive to SNR. Reconstruction rate 1 for signals with $N = 3$, $\Omega = 0.15$ and different SNR (30 dB and 10 dB) is achieved with the same number of the sampling channels (see Fig. 4(a) and 4(b)). In case of 1- and 2-band signals the reconstruction performance of other algorithms decrease to the M-OMP level when the signals have a low SNR (SNR$\leq$ 13 dB) (see Fig. 4(c)). In this case, in order to have the reconstruction rate equal to 1 with M-OMP, MUSIC and M-FOCUSS* the multi-coset scheme should have 9 channels.

We compare the reconstruction rates for the sampling patterns of different types. Plots on Fig. 5 shows that the reconstruction rate for the random and bunched sampling patterns is lower than for the sampling patterns obtained by the analysis of the condition numbers. Moreover, as can be seen on Fig. 5(a) the random sampling pattern for 12 sampling channels results in lower than expected reconstruction rate. This shows that relying on random selection of sampling patterns may lead to undesirable results.

Comparison of M-FOCUSS and M-BPDN is presented on Fig. 6. Reconstruction with M-BPDN results in lower RRMS error when $P < 6$, but in this case RRMS ≥ 0.8. This is a high reconstruction error that makes useless the reconstructed signal because it significantly differs from the input signal. Although the exact value of the acceptable RRMS error is defined by the specific application, we may assume that we are aiming to get RRMS not higher that 0.5. From this perspective M-FOCUSS has better reconstruction performance for all the test signals considered in this research.

V. Conclusions

This paper investigates the performance of commonly used reconstruction algorithms in discrete blind multi-coset sampling. Discrete multi-coset sampling can replace Nyquist-rate sampling in applications with frequency sparse signals.

Simulation results show that use of optimal sampling patterns results in the best reconstruction performance. Bunched

and random sampling patterns may lead to the undesirable decrease of the reconstruction performance.

When the number of non-zero slices is known prior to reconstruction, the modification of M-FOCUSS outperforms all other algorithms except for the low noise signals. In that case MUSIC is more beneficial. In order to use SA-MUSIC with the thresholding for the subspace estimation, the thresholding parameter should be picked for each type of a signal (number of bands, dynamic range, level of noise etc). M-OMP is a simple algorithm that can be successfully applied in case of signals with the small number of bands even with relatively high level of noise. M-FOCUSS and M-BPDN can be used when the number of non-zero slices of the DFT of the sequence of the samples of an input signal is not known prior to the reconstruction. In this case the M-FOCUSS algorithm also shows better performance.

References

[1] H. Landau, "Necessary density conditions for sampling and interpolation of certain entire functions," *Acta Mathematica*, vol. 117, pp. 37–52, 1967.

[2] P. Feng and Y. Bresler, "Spectrum-blind minimum-rate sampling and reconstruction of multiband signals," in *Conference Proceedings of IEEE International Conference on Acoustics, Speech, and Signal Processing, ICASSP-96*, vol. 3, May 1996, pp. 1688–1691.

[3] P. Vaidyanathan and V. Liu, "Efficient reconstruction of band-limited sequences from nonuniformly decimated versions by use of polyphase filter banks," *IEEE Transactions on Acoustics, Speech and Signal Processing*, vol. 38, no. 11, pp. 1927–1936, 1990.

[4] R. Vaughan, N. Scott, and D. White, "The theory of bandpass sampling," *IEEE Transactions on Signal Processing*, vol. 39, no. 9, pp. 1973–1984, sep 1991.

[5] M. Mishali and Y. C. Eldar, "Blind multiband signal reconstruction: Compressed sensing for analog signals," *IEEE Transactions on Signal Processing*, vol. 57, no. 3, pp. 993–1009, 2009.

[6] Y. Bresler, "Spectrum-blind sampling and compressive sensing for continuous-index signals," in *Information Theory and Applications Workshop, 2008*, Jan. 27 2008-Feb. 1 2008, pp. 547–554.

[7] M. Mishali, Y. Eldar, O. Dounaevsky, and E. Shoshan, "Xampling: Analog to digital at sub-Nyquist rates," *IET Circuits, Devices, Systems*, vol. 5, no. 1, pp. 8–20, 1 2011.

[8] K. Poulton, R. Neff, B. Setterberg, B. Wuppermann, T. Kopley, R. Jewett, J. Pernillo, C. Tan, and A. Montijo, "A 20 GS/s 8 b ADC with a 1 MB memory in 0.18 μm CMOS," in *IEEE International Solid-State Circuits Conference, ISSCC-2003. Digest of Technical Papers.*, vol. 1, Feb. 2003, pp. 318–496.

[9] S. Cotter, B. Rao, K. Engan, and K. Kreutz-Delgado, "Sparse solutions to linear inverse problems with multiple measurement vectors," *IEEE Transactions on Signal Processing*, vol. 53, no. 7, pp. 2477–2488, July 2005.

[10] K. Lee and Y. Bresler, "Subspace-augmented music for joint sparse recovery with any rank," in *IEEE Sensor Array and Multichannel Signal Processing Workshop (SAM), 2010*, Oct. 2010, pp. 205–208.

[11] E. van den Berg and M. P. Friedlander, "SPGL1: A solver for large-scale sparse reconstruction," June 2007, http://www.cs.ubc.ca/labs/scl/spgl1.

[12] ——, "Probing the Pareto frontier for basis pursuit solutions," *SIAM Journal on Scientific Computing*, vol. 31, no. 2, pp. 890–912, 2008.

[13] M. Mishali and Y. Eldar, "Reduce and boost: Recovering arbitrary sets of jointly sparse vectors," *IEEE Transactions on Signal Processing*, vol. 56, no. 10, pp. 4692–4702, Oct. 2008.

[14] E. J. Candès and M. B. Wakin, "An introduction to compressive sampling," *IEEE Signal Processing Magazine*, vol. 25, no. 2, pp. 21–30, Mar. 2008.